Corrosion mechanism and bioactivity of borate glasses analogue to Hench's bioglass

Mona A. Ouis[1], Amr M. Abdelghany[2,*], Hatem A. ElBatal[1]

[1]*Glass Research Department, National Research Center, 12311, Dokki, Cairo, Egypt*

[2]*Spectroscopy Department, National Research Center, 12311, Dokki, Cairo, Egypt*

Received 27 February 2012; received in revised form 23 April 2012; received in revised form 19 July 2012; accepted 23 July 2012

Abstract

Bioactive borate glasses (from the system Na_2O-CaO-B_2O_3-P_2O_5) and corresponding glass-ceramics as a new class of scaffold material were prepared by full replacement of SiO_2 with B_2O_3 in Hench patented bioactive glass. The prepared samples were investigated by differential thermal analysis (DTA), Fourier transform infrared (FTIR) spectroscopy and X-ray diffraction (XRD) analysis. The DTA data were used to find out the proper heat treatment temperatures for preparation of the appropriate glass-ceramics with high crystallinity. The prepared crystalline glass-ceramics derivatives were examined by XRD to identify the crystalline phases that were precipitated during controlled thermal treatment. The FTIR spectroscopy was used to justify the formation of hydroxyapatite as an indication of the bioactivity potential or activity of the studied ternary borate glasses or corresponding glass-ceramics after immersion in aqueous phosphate solution. The corrosion results are interpreted on the basis of suggested recent views on the corrosion mechanism of such modified borate glasses in relation to their composition and constitution.

Keywords*: borate bioactive glass, hydroxyapatite, IR spectroscopy, corrosion; X-ray diffraction*

I. Introduction

In recent years, research has focused on the development of new types of materials that stimulate a biochemical response from living tissue in order to obtain a strong chemical bond with biological fixation between the prosthesis and the tissue [1,2]. Bioactive modified soda lime silica glass 45S5 (Bioglass®) is the oldest bioactive material, first reported by Hench *et al*. in 1971 [3] and is now a very well-characterized material that has found use in a number of biomedical applications such as orthopedic implant and bone filler material [4–6].

To date, several glass compositions have been developed which have been demonstrated to be bioactive [7], a property that can be assessed by analyzing the formation of hydroxyapatite (HA) layer on the glass surfaces upon immersion in relevant physiological fluids. Most commercial bioactive glasses contain SiO_2 as a basic constituent. The mechanism of bonding in such silicate based bio- glasses involves partial dissolution due to presence of abundant modifier oxides which leads to the formation of a silica-gel layer and subsequent precipitation of a calcium phosphate layer [4,5]. Many authors have assumed that soluble silicon plays an important role in tissue repair and osteogenesis [4,5]. These statements are reached although of the fact that bones did not contain silicon ions in their constitution [8].

A new direction has begun towards the subsequent introduction of B_2O_3 replacing SiO_2 in the patented Hench's bioglass and investigation of the derived glasses showing acceptable bioactivity when immersed in simulated body fluid (SBF) [5,9]. Pure borate glasses have only recently explored for use in biomedical applications. Richard [10] was the first to investigate replacing SiO_2 with B_2O_3 in the 45S5 glass composition. The borate based 45S5 immersed in K_2HPO_4 solution at the body temperature (37 °C) formed a layer of hydroxyapatite [10] similar to that formed by the silicate based 45S5 when immersed in SBF. The in-vitro formation of HA from the borate based 45S5 glass led to further investigation in-vivo. Particles of the borate based 45S5 glass were placed in a rat tibial defect, and not only pro-

* Corresponding author: tel: +20 1 221133152
fax: +20 2 3370931, e-mail: *a.m_abdelghany@yahoo.com*

moted bone formation, but did so at a faster rate than the silicate based 45S5 glass [10]. The borate glass is fully converted to HA by the glass dissolution, i.e. by dissolving of B_2O_3 and Na_2O into solution and reacting of CaO with PO_4^{-3} from the phosphate solution. According to the mentioned results [10,11] the borate based glass is assumed to be most closely following a contracting volume type of behaviour, where the HA first forms at the outside of the glass particle, and then continually reacts inward toward the centre until completely reacted.

The main objective of this present work was to study the corrosion behaviour through the grain method of some prepared quaternary borate glass samples based on full substitution of B_2O_3 for SiO_2 in the Hench's patented Bioglass® and their glass-ceramics derivatives by the immersion in distilled water and sodium phosphate solution (Na_2HPO_4 0.25 M) for 1 hour at 90±2 °C. Also, two related glasses of higher B_2O_3 content in the same B_2O_3-Na_2O-CaO-P_2O_5 system were prepared and characterized. FTIR spectroscopic studies of the prepared samples before and after immersion in the phosphate solution were carried out to follow the structural evolution during the immersion process together with justifying the conversion of the prepared samples to hydroxyapatite as an indication of bioactivity. A further study in this work was to convert the prepared ternary borate glasses to their corresponding glass-ceramic derivatives and also to characterize the corrosion weight loss and bioactivity potential of glass-ceramic crystalline derivatives through following the formation of HA after immersion in the sodium phosphate solution. All these mentioned steps were also made for a Hench silicate patented glass 45S5 as a comparative reference material to the present work.

II. Experimental

The glasses were prepared from chemically pure grade materials with the compositions shown in Table 1. The precursor materials included quartz for SiO_2, H_3BO_3 for B_2O_3, anhydrous sodium and calcium carbonates for Na_2O and CaO, respectively. P_2O_5 was added in the form of ammonium dihydrogen phosphate ($NH_4H_2PO_4$). The weighed batches were melted in platinum crucible at 1100–1300 °C for 2 hours. The melts were rotated for 30 minutes and the homogenised melts were then cast into warmed stainless steel molds of the required dimensions. The prepared samples were immediately transferred to a muffle furnace, annealed at 400–450 °C for 1 hour and cool down to room temperature at a rate of 25 °C/h.

The glass-ceramics were obtained by thermal heat treatment of the prepared glass samples in two step regime at two different temperatures shown in Table 2. Each glass was firstly heated slowly (5 °C/min) to the nucleation temperature and hold for 6 hours (to form sufficient nuclei sites). After that, samples were further heated to the crystal growth temperature, hold 3 hours and left inside the muffle to cool down to room temperature at a rate of 20 °C/hour.

Differential thermal analysis (DTA) measurements, on Perkin Elmer DTA-7 apparatus, were carried out on the powdered glass samples which were examined up to 1000 °C using alumina powder as a reference material. The DTA data were used to find out the proper heat treatment temperatures for preparation of the appropriate glass-ceramic derivatives with high crystallinity.

Infrared absorption spectra of the bioglasses and their glass-ceramics derivatives were measured at room

Table 1. Chemical composition of the studied glasses

Glass No.	Composition [wt.%]				
	SiO_2	B_2O_3	Na_2O	CaO	P_2O_5
G1*	45	-	24.5	24.5	6.0
G2	-	45	24.5	24.5	6.0
G3	-	50	22.5	22.5	6.0
G4	-	55	19.5	19.5	6.0

*Hench bioglass

Table 2. Heat treatment conditions and corrosion weight loss of the investigated glasses and glass-ceramics

Glass No.	Thermal treatment		Weight loss [wt.%]	
	nucleation	crystal growth	in Na_2HPO_4 solution	in H_2O
G1*			2.20	7.84
G-C1*	550 °C/6 h	770 °C/3 h	1.17	5.60
G2			2.61	10.0
G-C2	500 °C/6 h	700 °C/3 h	1.32	8.80
G3			2.67	11.4
G-C3	500 °C/6 h	700 °C/3 h	1.79	10.9
G4			2.66	11.0
G-C4	500 °C/6 h	700 °C/3 h	1.62	10.9

*Hench bioglass

temperature (≈ 20 °C) in the wavenumber range 4000–400 cm^{-1} using a Fourier transform infrared spectrometer (type Mattson 5000, USA). Fine powder of the sample was mixed with KBr in the ratio 1 : 100 and the mixture was subjected to a load of 5 tons/cm^2 in an evacuated die to produce clear homogenous discs. Then, the IR absorption spectra were immediately measured after preparing the discs to avoid moister attack.

The glass-ceramic specimens were analysed by X-ray diffraction in order to identify the crystalline phases that precipitated during the heat treatment. The glass-ceramic samples were ground and examined using a Philips PW 1390 X-ray diffractometer with Ni-filtered CuKα radiation. The X-ray diffraction patterns were identified according to standard ASTM cards and recent related published data.

The chemical durability of the prepared bioglasses and their corresponding glass-ceramics was carried out using the grain method, which was adopted by several authors [9,12] and recommended by ASTM specifications. In the used method 1 g powdered glass sample (glass or glass-ceramic), having particle sizes in the range 0.16–0.25 mm, was accurately weighed in a sintered G4 Jena glass crucible, placed into polyethylene beaker (250 ml) and finally in water bath regulated at 90±2 °C. 150 ml of the distilled water was introduced to cover the powdered glass sample in polyethylene beaker in all cases for comparison and to avoid defects resulting from volumetric differences [13]. After 1 hour, the beaker was removed from the bath and the sintered glass crucible was connected to suction pump which pumped whole solution from the sample. The sintered glass crucible was transferred to an air oven at 120 °C for 1 hour, reweighed and finally the total weight loss was calculated. An empty sintered glass crucible of the same type (G4 Jena) was subjected to the same corrosion test condition and the obtained weight loss was taken into consideration. The same regime was used using disodium hydrogen phosphate (Na_2HPO_4) solution (0.25 M) to study and confirm the bone bonding ability. It is important to mention that in a similar study Day *et al* [1,11] used potassium phosphate (K_2HPO_4) solution to confirm the bioactivity potential of borate glasses.

III. Results and discussion

3.1 FTIR spectra of reference Hench bioglass

Figure 1 illustrates the FTIR absorption spectra of the reference Hench bioglass (G1) and its glass-ceramic derivative before and after immersion in sodium phosphate solution. The glass exhibits an infrared spectrum consisting of two medium bands at about 510 cm^{-1} and 750 cm^{-1} followed by a very broad band with two distinct peaks at about 960 and 1060 cm^{-1}. Also, the spectrum shows two small peaks at about 1460 and 1650 cm^{-1}. The IR spectrum shows in the near-region three small peaks at about 2680, 2800 and 2900 cm^{-1} and a final medium broad band centered at about 3440 cm^{-1}.

After immersion in sodium phosphate solution the IR spectrum of the base Hench bioglass was changed. Thus, the first two bands at 510 and 750 cm^{-1} decrease in intensity and are replaced by a double split band with two peaks at about 580 and 660 cm^{-1}. Also, the distinct peak at about 960 cm^{-1} is observed to disappear and a small peak is identified at about 890 cm^{-1}. Also, the small peak at about 1460 cm^{-1} becomes more prominent and show splitting to two peaks at about 1460 $cm^{-1}$and 1520 cm^{-1} and the peak at 1650 cm^{-1} remains prominent. The same FTIR spectral characteristics can be seen for the Hench bioglass-ceramic before and after immersion in sodium phosphate solution (Fig. 1).

3.2. FTIR spectra of borate glasses

Figure 2 illustrates the FTIR spectra of the prepared borate glasses before immersion in phosphate solution. It can be seen that the glass G2 containing the lowest

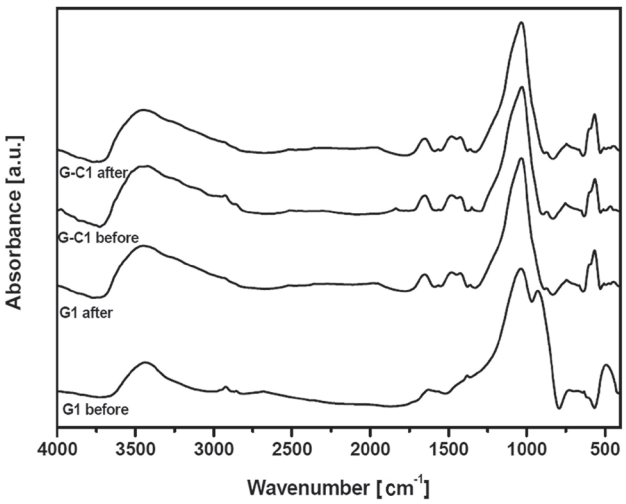

Figure 1. IR absorption spectra of Hench bioglass and bioglass-ceramic before and after immersion in sodium phosphate solution

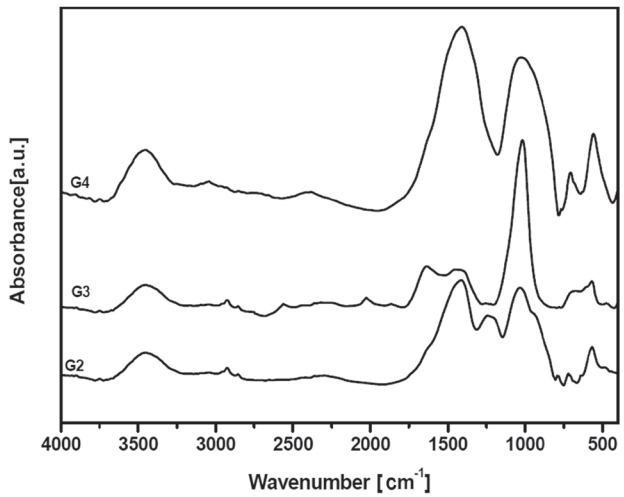

Figure 2. IR absorption spectra of prepared bioglasses before immersion in phosphate solution

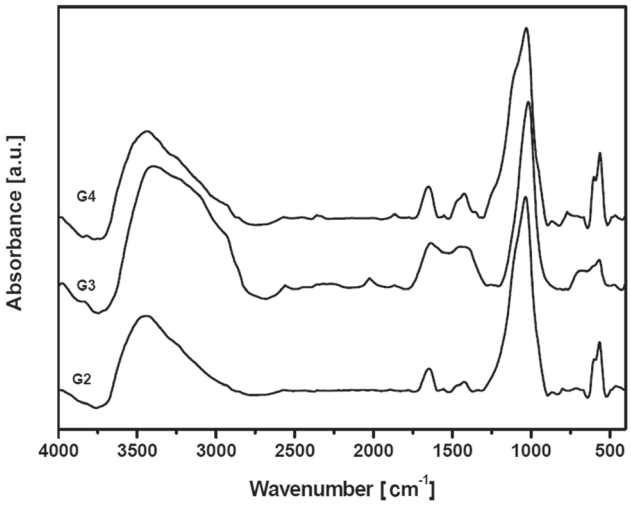

Figure 3. IR absorption spectra of prepared bioglasses after immersion in phosphate solution

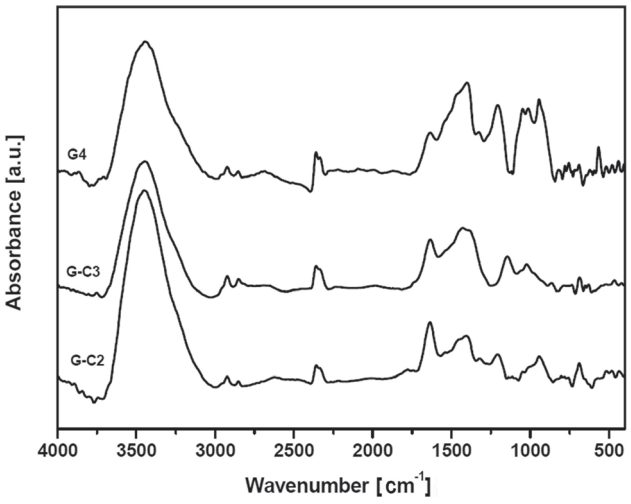

Figure 4. IR absorption spectra of prepared bioglass-ceramics before immersion in sodium phosphate solution

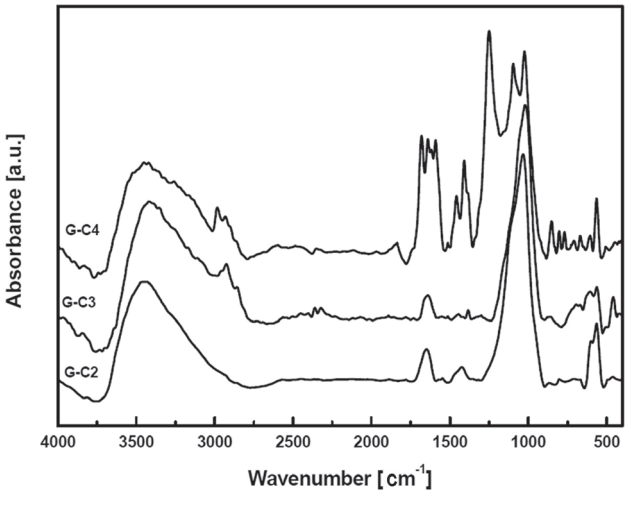

Figure 5. IR absorption spectra of prepared bioglass-ceramics after immersion in sodium phosphate solution

B_2O_3 content (45 wt.%) shows seven small peaks at about 640, 720, 770, 920, 1030, 1250, and 1430 cm^{-1} in the mid-region beside two small peaks at 2880 and 2920 cm^{-1} and a broad band centered at 3440 cm^{-1} in the near-infrared region. In comparison to the glass G2 the FTIR spectra of the glasses G3 and G4 show two broad and highly prominent bands with peaks at about 1150 and 1500 cm^{-1}. The rest of the peaks are very similar with corresponding FTIR bands of the sample G2.

Figure 3 illustrates the FTIR spectra of the prepared borate glasses after immersion in the phosphate solution. The spectral features can be characterized with: a small peak at about 510 cm^{-1}, a sodium broad band with two peaks at about 580 and 680 cm^{-1}, a distinct broad and sharp band at about 1060 cm^{-1}, the decreased intensity of the absorption bands within the region 1200–1500 cm^{-1} and the increased intensity of the very broad band centered at about 3450 cm^{-1}.

3.3. FTIR spectra of borate glass-ceramics

Figure 4 illustrates the FTIR spectra of the prepared glass-ceramics before immersion in sodium phosphate solution. It is evident that IR spectra reveal numerous sharp characteristic peaks representing well crystallised phases. Also, it is observed that for the glass-ceramics G-C2 and G-C3 the IR absorption bands within the region 1200–1600 cm^{-1} have relatively higher intensities than the bands in the region 800–1200 cm^{-1}.

Figure 5 shows the FTIR spectra of glass-ceramic derivatives after immersion in the sodium phosphate solution at 90±2 °C for 1 h. The IR spectra reveal the appearance of various characteristic bands due to trigonal and tetrahedral borate groups: a small peak at about 500 cm^{-1}, two distinct peaks at 566 and 603 cm^{-1}, two small bands at 698 and 804 cm^{-1}, two medium bands at 1423 and 1643 cm^{-1}, a very broad band centred at 3450 cm^{-1}. The samples G-C2 and G-C3 exhibit almost the same IR spectra as their parent glasses after immersion (Figs. 3 and 5). Exception is the sample GC4 with the highest B_2O_3 content (55 wt.%) as its FTIR spectrum is characterized by splitting in the mid-infrared region. Thus, three distinct peaks at about 1080, 1150, and 1250 cm^{-1} and two medium bands at about 1460 and 1650 cm^{-1} can be clearly seen in Fig. 5.

3.4. X-ray diffraction data

Figures 6 and 7 illustrate the X-ray diffraction patterns of the prepared heat-treated glass-ceramics derivatives. The glass-ceramic G-C1 prepared from the Hench's bioglass consists of sodium calcium silicate solid solution ($3Na_2O{\cdot}3CaO{\cdot}6SiO_2$ or $Na_6Ca_3Si_6O_{18}$) as the main crystalline phase. In the borate glass-ceramic G-C2 the following crystalline phases were detected: calcium sodium borate ($CaNa_3B_5O_{10}$) 34.5% with triclinic structure, calcium phosphate (CaP_2O_6) and boron calcium oxide ($B_2Ca_2O_5$) 31.1% with monoclinic structure. The borate glass-ceramic G-C3 has sim-

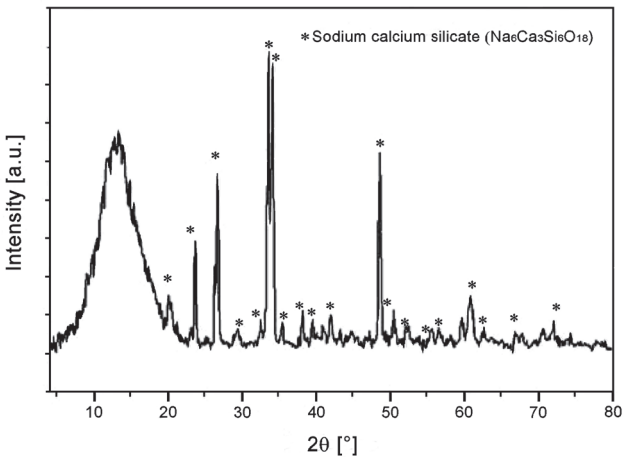

Figure 6. X-ray pattern of Hench bioglass

ilar XRD pattern, but the following crystalline phases can be identified: sodium phosphate ($Na_5P_3O_{10}$) 32.9% with monoclinic structure, calcium sodium borate ($CaNa_3B_5O_{10}$) 24.7% with triclinic structure, boron calcium oxide ($B_2Ca_2O_5$) 22.2% with monoclinic structure, calcium phosphate (CaP_4O_{11}) 10.9% with monoclinic structure and calcium phosphate (CaP_2O_6) 9.3%. The borate glass-ceramic G-C4 with the highest boron content has somewhat different crystalline structure and contains: calcium borate (CaB_2O_4) 37.3% with orthorhombic structure, calcium phosphate ($Ca_2P_2O_7$) 31.3% and sodium phosphate ($NaPO_3$) 31.3% with monoclinic structure.

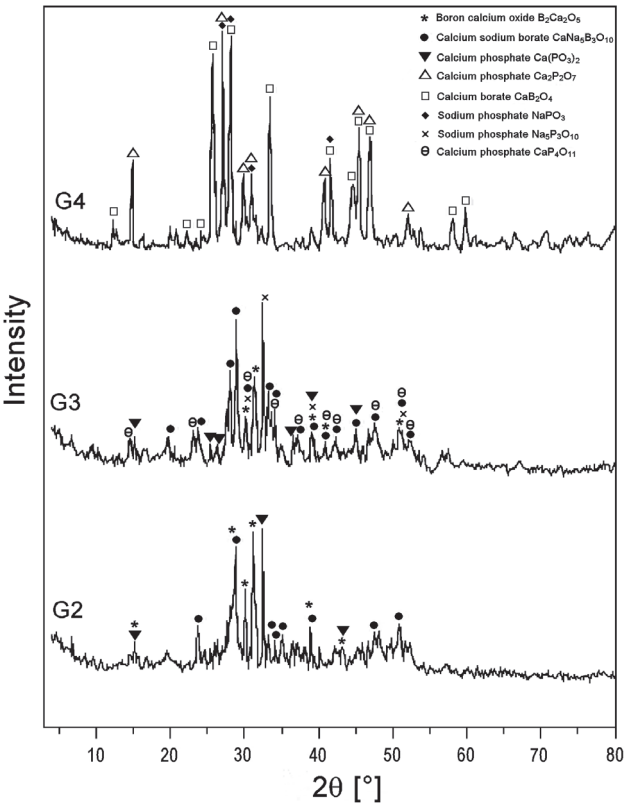

Figure 7. X-ray pattern of prepared bioglass-ceramics

3.5. Corrosion results

Table 2 depicts the corrosion behaviour of the studied glasses and glass-ceramics. The weight losses of all the borate glasses immersed in sodium phosphate solution are slightly higher than that obtained from the Hench bioglass. However, the weight losses due to corrosion have only slight increase with the increase of B_2O_3 content. The glass-ceramic derivatives of all the samples reveal lower corrosion durability in comparison to their parent glasses. In addition, the corrosion in distilled water is considerably higher than in sodium phosphate solution.

IV. Discussion

4.1. Interpretation of FTIR results

Analysis of the vibrational spectra can provide useful structural information [14,31] about glass constitution and also to identify the presence of defect centers or radiation-induced defects [15,16], the presence of low-concentration impurities such as water, hydroxyle etc. [17] or the formation of hydroxyapatite surface layer on the bioglass after immersion in specific SBF or even phosphate solution [18–20]. It is accepted that the main vibrational modes associated with the glass network mostly appear above 500 cm^{-1} in the mid-infrared region [21–23]. The atomic arrangement in glass leads to the development of structure with considerable short range order on a scale nearest neighbour interatomic distances [24]. X-ray analysis fails to identify the constitutional structural units within the glass while FTIR measurements are accepted to be able to give valuable information of the glass constitution in comparison with related crystalline counterpart [17–25].

Before detailed assignments of the vibrational modes of the experimental results of the studied soda lime borate glasses with constant P_2O_5 content, the concept introduced by Tarte [25] and Condrate [26] should be adopted and taken into consideration. In a vitreous system, it is assumed that vibrations of the characteristic groups of atoms in the network are independent of the vibrations of other groups. Regarding the borate glasses, the vibrational structural modes are generally accepted to be active in three infrared spectral regions [21–23]:

- 1200–1500 cm^{-1} - originates from B-O stretching vibrations of trigonal BO_3 units,
- 850–1200 cm^{-1} - due to B-O stretching vibrations of tetrahedral BO_4 units,
- 600–800 cm^{-1} - belongs to bending vibrations of various borate segments.

The basic composition of the studied modified borate glasses consists of main constituent of B_2O_3 (45–55 wt.%) and with constant P_2O_5 (6 wt.%). Thus, it is expected that the vibrational modes are mainly due to different borate units (triangular and tetrahedral borates) besides the sharing of some few phosphate groups. The two mixed glass building units superimpose with each other but the vibrations due to borate units are predominating.

The experimental FTIR spectrum of the reference Hench bioglass (Fig. 1), consisting of mixed main silicate (45 wt.% SiO_2) network and partner phosphate (6 wt.% P_2O_5) network, exhibit mainly vibrations assigned as follows [13–23]:

- the Si-O bending mode is located in the range 450–510 cm^{-1} and 670–740 cm^{-1},
- the band between 890 and 970 cm^{-1} is associated with the $Si\text{-}O^-$ with one non-bridging oxygen,
- the Si-O stretching mode is located in the range 1000–1200 cm^{-1},
- the band at about 1460 cm^{-1} is due to carbonate group,
- the band around 1640 cm^{-1} is related to molecular water,
- the bands at about 2820, 2928, and 3450 cm^{-1} are related to different modes of water, OH or silanol groups.

The contributions of the phosphate network, as a second component, are being mostly overlapped by the bands due to main silicate network and are not separated as individual IR vibrations. The IR spectra of the Hench's bioglass and the corresponding glass-ceramic after immersion in sodium phosphate solution reveal two important changes (Fig. 1). The first change is the disappearance of the band at 890–970 cm^{-1}. This specific band is related to $Si\text{-}O^-$ and this confirms the proposed ion exchange process for corrosion in this type of modified soda lime silica glass and the replacement of ($Si\text{-}O^-\ Na^+$) by (Si-OH) [18]. The second change is the appearance of the double split band with two peaks at about 580 and 620 cm^{-1} indicating the formation of hydroxyapatite [18].

The IR absorption spectra of the studied borate glasses before immersion (Fig. 2) reveal vibrational bands which are characteristic of borate network consisting of triangular (BO_3) and tetrahedral (BO_4) groups composed of units such as diborates, pertaborates, and triborates. The asymmetric stretching vibrations of tetrahedral borate units are seen to be active within the range 800–1200 cm^{-1} as evidenced by the appearance of the strong bands at about 1050 and 950 cm^{-1}. The high frequency absorption at 1200–1550 cm^{-1} can be related to triangular units (BO_3 and BO_2O^-), which are absorbing at this region. The low frequency part of the mid-region (500–800 cm^{-1}) is dominated by the bending vibrations or deformation modes of various borate units, and the bands around 700 cm^{-1} represent this mode. The peaks within the range 400–580 cm^{-1} are assumed by some authors [27,28] to represent vibrations of modifier cations (Na^+, Ca^{2+}) in these glasses.

The IR absorption spectra of the studied borate glasses after immersion in sodium phosphate solution (Fig. 3) reveal three important changes in the spectra. The strong persistence of the main band at about 1050 cm^{-1} and the quite decrease of the intensities of the bands in the region 1250–1500 cm^{-1} which indicate that the bands due to BO_3 vibrations highly decrease but the bands due to BO_4 persist and remain prominent. Also, identification of a new band with two split peaks at about 560 and 620 cm^{-1} confirms the formation of hydroxyapatite [18].

The FTIR of glass-ceramics before immersion (Fig. 4) reveal numerous bands within the mid-region which indicate that the vibrations are due to fine-grained crystalline phases formed during controlled crystallisation of the original base glasses. The IR spectra of the glass-ceramics after immersion in the diluted phosphate solution (Fig. 5) show the resolution of the far-infrared band with two split peaks at about 560 and 620 cm^{-1} confirming the formation of hydroxyapattite crystals. Also, the two glass-ceramics with 45 and 50 wt.% B_2O_3 reveal the persistence of the main band at about 1050 cm^{-1} while the glass-ceramic sample containing 55 wt.% B_2O_3 reveals the extension of the mid-bands within the region 1050–1600 cm^{-1} showing several high intense bands with split peaks. This last sample (GC4) reveals that both triangular and tetrahedral borate units are highly persistent upon crystallisation of the glass containing 55 wt.% B_2O_3 and also after immersion. It seems that the various crystalline species formed are quite resistant to the action of dilute phosphate solution as expected from the glass-ceramic derivative.

4.2. Interpretation of the corrosion results

The corrosion of patented Hench's bioglass is agreed upon to be similar to traditional commercial silicate glasses involving hydration and ion-exchange processes between the modifier alkali cations from glass and hydrogen or hydronium ions from the contact solution [18,28]. The rate of corrosion in this specific Hench's bioglass is rapid due to the presence of substantial amounts of both modifiers: alkali oxide (24.5 wt.% Na_2O) and alkaline earth oxide (24.5 wt.% CaO). The modifier ions are present in network modifying positions and their cations are loosely bound and can be easily detached during leaching by the action of dilute phosphate solution. Two equations have been proposed [18,28] to express the mechanism of corrosion in Hench's bioglass:

$$\equiv Si\text{-}O\text{-}R + H_3O \rightarrow \equiv Si\text{-}OH + R^+ + H_2O \quad (1)$$

$$\equiv Si\text{-}O\text{-}R + H_2O \rightarrow \equiv Si\text{-}OH + R^+ + OH \quad (2)$$

The third suggested mechanism is given for silicate network dissolution:

$$\equiv Si\text{-}O\text{-}Si(OH) + 3\ (OH)^- \rightarrow \equiv Si\text{-}O\text{-}Si\ (OH)^-_4 \rightarrow \equiv Si\text{-}O^- + Si(OH)_4 \quad (3)$$

The further suggested reaction associated after the formation of surface SiO_2 gel is the condensation of the silanol (SiOH) groups as follows:

$$Si\text{-}OH + HO\text{-}Si \rightarrow Si\text{-}O\text{-}Si + H_2O \quad (4)$$

The corrosion mechanism of alkali-alkaline earth borate glasses is eventually quite different from that for

alkali-alkaline earth silicate glasses because almost all the glass components within the studied borate glasses are dissolved in aqueous solutions but with somewhat different degrees. Velez *et al.* [29] have assumed that the corrosion of borate glasses proceeds through a dissolution process which takes place by a situation controlled mechanism and not by ion-exchange process which is a distinctive way for silicate corrosion. B_2O_3, Na_2O, and P_2O_5 are easily released components from borate glass and are rapidly dissolved because of their known strong ability to dissolve in aqueous media by a measurable degree [19,20]. CaO is known to be less soluble than the mentioned other constituents and can form sparingly soluble $Ca(OH)_2$ or to be in contact with phosphate cations from the leaching solution or from the glass and thus forms calcium phosphate with the final pathway to be converted to hydroxyapatite. The experimental FTIR spectra (Fig. 3) indicate that the vibrational bands within the region 1200–1500 cm^{-1} are observed to decrease in intensity with a measurable degree after immersion in dilute phosphate solution. This result can be interpreted by assuming that the triangular borate units are primarily easily dissolved while the compact tetrahedral borate units are relatively stable and less soluble and hence their vibrations are observed to be persistent. Previous studies on alkali borate glasses support this assumption [19,20,30].

The corrosion of glass-ceramics derivatives can be realised and understood by assuming that the precipitated or formed crystalline species are also easily hydrolysed and dissolved in the same procedure suggested for the present glasses. The only exception is the glass G4 containing 55 wt.% B_2O_3, as the FTIR spectrum after corrosion (Fig. 5) indicates that the crystalline species are stable, most probably due to the presence of relatively high percent of more stronger BO_4 units. The observed results can initiate further investigation to find out detailed behaviour of borate glasses with higher B_2O_3 contents. X-ray diffraction data of the glass-ceramic G4 (Fig. 7) indicate that the formed phases are somewhat different than in the glass-ceramics G2 and G3. The main phases in the sample G4 are calcium phosphate and calciborite while in the samples G2 and G3 the calcium sodium borate phase is predominant. This may explain the difference in corrosion behaviour as revealed by FTIR results.

The result of high solubility with distilled water can be attributed to the free dissolving ability of clear distilled water without any dissolved constituents while sodium phosphate solution seems to possess the liability to dissolve the basic constituents more than the acidic constituent because the phosphate anion is more acidic than borate or silicate anions. This behaviour needs still more studies to confirm the corrosion route.

4.3. Interpretation of the X-ray data

Experimental X-ray measurements indicate the formation of microcrystalline phases after controlled thermal treatment of the studied bioglasses (as shown in Figs. 6 and 7). It is generally accepted that the type of the formed microcrystalline phases depends on both the composition of the bioglass and heat-treatment conditions [31–33]. The Hench silicate bioglass (45S5) can easily crystallise and forms a main phase of sodium calcium silicate solid solution. It has been assumed [34,35] that the reason is the presence of both silicate and phosphate networks together and the possibility of obvious phase separation upon thermal treatment. It is accepted by various scientists [34–36] that the addition of P_2O_5 (even a few percent) to silicate glass network promotes volume nucleation and crystallisation. There is some evidence that precipitated phosphate crystals subsequently act as heterogeneous nucleation sites for the formation of major phases, although the detailed role of P_2O_5 remains debatable [31–36].

Regarding the modified Hench glass from the system (Na_2O-CaO-SiO_2-P_2O_5), Masterlrao *et al*. [37] have confirmed by EXAFS measurements that there is a relationship between the short-range order around the modifier cations and the crystal nucleation tendency in the silicate glasses of the two systems (SiO_2-CaO-Na_2O) and (SiO_2-CaO). Glasses of these two systems can easily nucleate in the volume because they have similar local structure to their isochemical crystalline phases. Publications on a similar background about Na_2O-CaO-B_2O_3 and CaO-B_2O_3 are lacking and extensive studies of the tendency on crystallisation in borate glasses are still needed by recent techniques.

The interpretation of the X-ray diffraction patterns data (Fig. 7) can be summarized as follows:

a) In all borate glass-ceramics calcium phosphate is one of the phases precipitated or formed during thermal treatment. This result supports the assumption of Hudon and Baker [38,39] about the ability of Ca^{2+} ions to participate in phase separation in borate glass and to form with P_2O_5 calcium phosphate phase.
b) In all borate glass-ceramics another main phase of calcium borate type with different formula was observed. This result also confirms the assumption of Hudon and Baker [38,39] about the readiness of Ca^{2+} to nucleate and form crystalline phase.
c) Ternary calcium-sodium-borate crystalline phase is the major phase formed after thermal treatment of the glass G2, the second phase in the glass-ceramic G-C3, but not identified in the sample G-C4. This behaviour can be correlated with the percents of all the three constituents (Na_2O, CaO, B_2O_3), i.e. with increasing the B_2O_3 from 45 wt.% to 55 wt.% the modifier oxide (Na_2O and CaO) content decreases from 24.5 to 19.5 wt.% (Table 1).

d) The glass-ceramics prepared from glasses with higher B_2O_3 content (the glasses G3 and G4) contain a crystalline sodium phosphate phase. This phase formation is expected as the other constituent components have shared in the formation of other crystalline phases.

V. Conclusions

A comparative corrosion and bioactivity studies of some prepared borate glasses of the analogue composition to silicate Hench bioactive glass by full replacement of SiO_2 by B_2O_3 have been carried out. The studied borate glasses analogous to Hench bioglass reveal by FTIR analysis the formation of characteristic peaks due to hydroxyapatite after immersion in a sodium phosphate solution for 1 hour at 90±2 °C. It is observed that the bioactivity potential slightly decreases with increasing the B_2O_3 from 45 to 55 wt.%. The glass-ceramic derivatives prepared by controlled heat treatment reveal similar bioactivity to the parent glasses. A proposed corrosion mechanism is introduced to interpret the ease dissolution behaviour of borate glasses which is different from the ion exchange process in silicate glasses including Hench's bioglass. The difference in corrosion behaviour of distilled water and diluted sodium phosphate solution is related to the clearness of distilled water from any dissolving ions and hence more dissolving power of distilled water to all constituents. However, sodium phosphate is proposed to dissolve alkali constituents better than acidic borate matrix. This effect needs further and continuous studies.

References

1. W. Liang, M.N. Rahaman, D.E. Day, N.W. Marion, G.C. Riley, J.J. Mao, "Bioactive borate glass scaffold for bone tissue engineering", *J. Non-Cryst. Solids*, **354** (2008) 1690–1696.
2. C.R. Mariappan, D.M. Yunos, A.R. Boccaccini, B. Roling, "Bioactivity of electro-thermally poled bioactive silicate glass", *Acta Biomater.*, **5** [4] (2009) 1274–1283.
3. L.L. Hench, R.J. Splinter, W.C. Allen, T.K. Greenlee, "Bonding mechanisms at the interface of ceramic prosthetic materials", *J. Biomed. Mater. Res.*, **5** [6] (1972) 117–141.
4. W. Cao, L.L. Hench, "Bioactive materials", *Ceram. Int.*, **22** [6] (1996) 493–507.
5. L.L. Hench, "Bioceramics, a clinical success", *J. Am. Ceram. Soc.*, **81** [7] (1998) 1705–1727.
6. R.M. Day, A.R. Boccaccini, S. Shurey, J.A. Roether, A. Forbes, L.L. Hench, S.M. Gabe. "Assessment of polyglycolic acid mesh and bioactive glass for soft-tissue engineering scaffolds", *Biomater.*, **25** [27] (2004) 5857–5866.
7. S.R. Moosvi, R.M. Day, "Bioactive glass modulation of intestinal epithelial cell restitution", *Acta Biomater.*, **5** [1] (2009) 76–83.
8. A. Ravaglioli, A. Krajewski, p. 17 in *Bioceramics: Materials, properties, applications*, Chapman & Hall, London, 1992.
9. K.M. ElBadry, F.A. Moustafa, M.A. Azooz, F.H. El-Batal, "Corrosion behaviour of some selected bioglasses by different aqueous solutions", *Glass Technol.*, **43** [4] (2002) 162–170.
10. M.N.C. Richard, *Bioactive behavior of a borate glass, MS Thesis*, University of Missouri-Rolla 2000.
11. S.B. Jung, D.E. Day, "Conversion kinetics of silicate, borosilicate, and borate bioactive glasses to hydroxyapatite", *Phys. Chem. Glasses: Eur. J. Glass Sci. Technol. B*, **50** [2] (2009) 85–88.
12. A.A. Khedr, H.A. ElBatal, "Corrosion of zinc-containing cabal glasses by various leaching solutions", *J. Am. Ceram. Soc*., **79** [3] (1996) 733–741.
13. J. Hlavac, p. 188 in *The Technology of Glass and Ceramics, Glass Science and Technology, 4*, Elsevier Scientific Publishing Company, Amsterdam, 1983.
14. N.B. Colthup, L.H. Daly, S.E. Wiberley, *Introduction to infrared and Raman spectroscopy*, 3rd ed. Academic Press, New York, 1990.
15. F.H. ElBatal, S.Y. Marzouk, N. Nada, S.A. Desouky, "Optical properties of vanadium-doped bismuth borate glasses before and after gamma-ray irradiation", *Philos. Magaz.*, **90** [6] (2010) 675–677.
16. H.A. ElBatal, A.M. Abdelghany, F.H. ElBatal, Kh.M. ElBadry, F.A. Moustaffa, "UV-visible and infrared absorption spectra of gamma irradiated CuO-doped lithium phosphate, lead phosphate and zinc phosphate glasses: A comparative study", *Physica B*, **406** [9] (2011) 3694–3703.
17. R.D. Husung, R.H. Doremus, "Infrared transmission spectra of four silicate glasses before and after exposure to water", *J. Mater. Res.*, **5** [10] (1990) 2209–2217.
18. F.H. ElBatal, A.A. ElKheshen, "Preparation and characterization of some substituted bioglasses and their ceramic derivatives from the system SiO_2-Na_2O-CaO-P_2O_5 and effect of gamma irradiation", *Mater. Chem. Phys.*, **110** (2008) 352–362.
19. A.M. Abdelghany, H.A. ElBatal, F.M. EzzElDin, "Bone bonding ability behavior of some ternary borate glasses by immersion in sodium phosphate solution", *Ceram. Int.*, **38** (2012) 1105–1113.
20. A.M. Abdelghany, "Novel method for early investigation of bioactivity in different borate bioglass", *Spectrochimica Acta A*, DOI:10.1016/j.saa.2012.02.051.
21. E.I. Kamitsos, A.P. Patsis, M.A. Kaskassides, G.D. Chryssikos, "Infrared reflectance spectra of lithium borate glasses", J. *Non-Cryst. Solids*, **126** (1990) 52–67.
22. E.I. Kamitsos, G.D. Chryssikos, "Alkali sites in glass", *Solid State Ionics*, **105** (1998) 75–85.
23. E.I. Kamitsos, "Infrared studies of borate glasses", *Phys. Chem. Glasses*, **44** (2003) 79–87.
24. P.H. Gaskell, pp. 175–278 in *Materials Science and Technology, Vol. 9*, Ed. J. Zarzycki, VCH, Weinheim, Germany, 1991.

25. P. Tarte, "Identification of Li-O bands in the infra-red spectra of simple lithium compounds containing LiO_4 tetrahedra", *Spectrochimica Acta*, **20** (1964) 238–240.
26. R. Condrate, p. 101 in *Introduction to Glass Science*, Plenum, New York, 1972.
27. B.N. Nelson, G.J. Exarhos, "Vibrational spectroscopy of cation site interactions in phosphate glasses", *J. Chem. Phys.*, **71** (1979) 2739–2748.
28. K.M. ElBadry, F.A. Moustafa, M.A. Azooz, F.H. El-Batal, "Corrosion behaviour of some bioglasses towards different leaching solutions", *Glass Technol.*, **43** [4] (2002) 162–170.
29. M.H. Velez, H.L. Tuller, D.R. Uhlmann. "Chemical durability of lithium borate glasses", *J. Non-Cryst. Solids*, **49** [1-3] (1982) 351–361.
30. N.A. ElAlaily, F.M. Ezz ElDin, H.A. ElBatal, "Durability of some gamma-irradiated alkali borate glasses", *Radiat. Phys. Chem.*, **44** (1994) 45–51.
31. M.M. Sebdani, M.H. Fathi, "Novel hydroxyapatite-forsterite-bioglass nanocomposite coatings with improved mechanical properties", *J. Alloys Comp.*, **509** (2011) 2273–2276.
32. O.P. Filho, G.P. La Torre, L.L. Hench, "Effect of crystallization on apatite-layer formation of bioactive glass 45S5", *J. Biomed. Mater. Res.*, **30** (1996) 509–514.
33. O. Peitl, E.D. Zanotto, L.L. Hench, "Highly bioactive P_2O_5-Na_2O-CaO-SiO_2 glass-ceramics", *J. Non-Cryst. Solids*, **292** [1-3] (2001) 115–126.
34. P.W. McMillan, *Glass-Ceramics*, 2nd ed., Academic Press, London, 1979.
35. P.F. James, Chapter 3:59 in *Glasses and Glass-Ceramics*, ed. M.H. Lewis, Chapman and Hall, London, 1989.
36. P.F. James, "Glass ceramics: new compositions and uses", *J. Non-Cryst. Solids*, **181** (1995) 1–15.
37. V.R. Mastelaro, E.D. Zanotto, N. Lequeux, R. Cortes, "Relationship between short-range order and ease of nucleation in $Na_2Ca_2Si_3O_9$, $CaSiO_3$ and $PbSiO_3$ glasses", *J. Non-Cryst. Solids*, **262** (2000) 191–199.
38. P, Hudon, D.R Baker, "The nature of phase separation in binary oxide melts and glasses. I. Silicate systems", *J. Non-Cryst. Solids*, **303** [3] (2002) 299–345.
39. P. Hudon, D.R. Baker, "The nature of phase separation in binary oxide melts and glasses. II. Selective solution mechanism", **303** [3] (2002) 346–353.